The EMBO Journal Vol.16 No.7 pp.1531–1540, 1997

Identification of two regions in the N-terminal domain of ActA involved in the actin comet tail formation by *Listeria monocytogenes*

Iñigo Lasa, Edith Gouin, Mark Goethals[1], Katia Vancompernolle[1], Violaine David, Joël Vandekerckhove[1] and Pascale Cossart[2]

Unité des Interactions Bactéries-Cellules, Institut Pasteur, 28 rue du Docteur Roux, 75724 Paris, France and [1]Flanders Interuniversity Institute for Biotechnology, Department of Biochemistry, Faculty of Medicine, University of Ghent, B-9000 Ghent, Belgium

[2]Corresponding author

The ActA protein of *Listeria monocytogenes* induces actin nucleation on the bacterial surface. The continuous process of actin filament elongation provides the driving force for bacterial propulsion in infected cells or cytoplasmic extracts. Here, by fusing the N-terminus of ActA (residues 1–234) to the ω fragment of β-galactosidase, we present the first evidence that this domain contains all the necessary elements for actin tail formation. A detailed analysis of ActA variants, in which small fragments of the N-terminal region were deleted, allowed the identification of two critical regions. Both are required to initiate the actin polymerization process, but each has in addition a specific role to maintain the dynamics of the process. The first region (region T, amino acids 117–121) is critical for filament elongation, as shown by the absence of actin tail in a 117–121 deletion mutant or when motility assays are performed in the presence of anti-region T antibodies. The second region (region C, amino acids 21–97), is more specifically involved in maintenance of the continuity of the process, probably by F-actin binding or prevention of barbed end capping, as strongly suggested by both a deletion (21–97) leading to 'discontinuous' actin tail formation and *in vitro* experiments showing that a synthetic peptide covering residues 33–74 can interact with F-actin. Our results provide the first insights in the molecular dissection of the actin polymerization process induced by the N-terminal domain of ActA.

Keywords: ActA/actin polymerization/actin tail/intracellular movement/*Listeria monocytogenes*

Introduction

Several unrelated intracellular bacterial pathogens, including *Listeria monocytogenes*, *Listeria ivanovii*, *Shigella flexneri* and some *Rickettsiae*, share the ability to use actin polymerization as a driving force for intracellular movement, cell-to-cell spread and dissemination within infected tissues (for review, see Lasa and Cossart, 1996). Recently, vaccinia virus has also been shown to move through the host cell cytoplasm in association with an actin tail (Cudmore *et al.*, 1995). The actin dynamics involved in the propulsive movement of these pathogens has striking similarities with the protrusion of lamellipodia in locomoting cells, providing a simple and powerful model to understand the actin assembly at the plasma membrane of motile cells.

The proteins responsible for actin-based movement of *L.monocytogenes*, *L.ivanovii* and *S.flexneri* (ActA, IactA and IcsA, respectively) have been identified (Lett *et al.*, 1989; Domann *et al.*, 1992; Kocks *et al.*, 1992; Gouin *et al.*, 1995; Kreft *et al.*, 1995). The overall homology between ActA and IactA is not high (39% identity) and there is no detectable sequence homology between ActA and IcsA. However, converging data suggest that these proteins may interact at different levels of a common pathway leading to actin assembly (for reviews, see Cossart, 1995; Theriot, 1995; Lasa and Cossart, 1996).

ActA is a surface protein of 639 amino acids which is anchored to the bacterial membrane (Domann *et al.*, 1992; Kocks *et al.*, 1992). Several lines of evidence demonstrate that ActA is the bacterial factor responsible for actin-based motility. First, ActA-deficient mutant strains do not polymerize actin (Domann *et al.*, 1992; Kocks *et al.*, 1992). Second, wild-type ActA, when expressed in mammalian cells, is targeted to mitochondria ('mitochondrial targeting assay'), which become covered with actin filaments (Pistor *et al.*, 1994). Similarly, when ActA is fused to the plasma membrane anchor sequence of K-ras (CAAX-box), it induces actin polymerization at the inner face of the plasma membrane and changes in cell morphology (Friederich *et al.*, 1995). Third, heterologous expression of ActA in the non-pathogenic bacterium *Listeria innocua* (Kocks *et al.*, 1995), or binding of a recombinant ActA protein to the surface of *Streptococcus pneumoniae* (Smith *et al.*, 1995) are sufficient to produce comet tails and actin-based motility in *Xenopus* extracts (Theriot *et al.*, 1994).

Due to the presence of a proline-rich repeats region in the central part of the protein, ActA has been artificially divided into three domains: (i) an N-terminal domain (1–234; numbering of amino acids as described by Kocks *et al.*, 1992); (ii) the proline-rich repeats region (235–395); and (iii) the C-terminal domain (396–585; Lasa *et al.*, 1995). Sequence analysis of ActA revealed that the proline-rich repeats and the C-terminal domain share significant sequence similarities with zyxin, an actin-binding protein associated with focal contacts and stress fibres (R.Goldstein, E.Friederich and D.Louvard, personal communication). In contrast, the N-terminal domain of ActA is not similar to known proteins, and only small motifs, either similar to the presumptive actin binding site of caldesmon (64-LKEKAE-70) or present in the cofilin-ADP protein family (115-EIKKRRKA-122), can be detected.

The mechanism by which ActA induces actin polymerization remains an open question. Attempts to demonstrate *in vitro* interactions between ActA and G-actin have failed (Kocks *et al.*, 1992) and *Listeria* grown in broth do not

nucleate actin efficiently (Tilney *et al.*, 1992). Microinjection of fluorescently labelled phalloidin in infected cells (Sanger *et al.*, 1995), or treatment of cytoplasmic extracts of *Xenopus* eggs with phalloidin (Marchand *et al.*, 1995), causing polymerization of endogenous G-actin, have suggested that bacteria do not recruit preformed actin filaments to the actin tail. Thermodynamic studies of *L.monocytogenes* motility in *Xenopus* extracts support the view that actin assembly results from the local maintenance of uncapped filament barbed ends at the bacterium surface (Marchand *et al.*, 1995). These observations can be explained by considering either that ActA recruits one or more host proteins responsible for the nucleation and filament uncapping activities, or that modification of ActA inside cells gives this protein the ability to possess these activities. Several actin-binding proteins (α-actinin, tropomyosin, fimbrin, talin, villin, profilin, VASP and vinculin) have been localized to the comet tails or at the rear of the bacteria, where actin polymerization occurs (for review, see Cossart, 1995). Among these proteins only VASP (vasodilator-stimulated phosphoprotein) is able to bind purified ActA (Chakraborty *et al.*, 1995). VASP also interacts with profilin (Reinhard *et al.*, 1995), a 15.5 kDa protein that plays a key role in actin polymerization (Pantaloni and Carlier, 1993).

In a previous study (Lasa *et al.*, 1995), we generated several *L.monocytogenes* strains expressing ActA protein variants. Analysis of these strains demonstrated that: (i) deletion of the N-terminal domain inhibits actin tail formation; (ii) deletion of the proline-rich repeats decreases the speed of movement, but actin tails are still formed; and (iii) deletion of the C-terminal domain has no effect on actin-based motility. Since VASP binds to the proline-rich repeats of ActA (Pistor *et al.*, 1995; also our unpublished results), these data suggested that profilin bound to VASP could provide polymerization-competent actin monomers, and thereby increase the efficiency of the ActA-mediated actin polymerization process, but that VASP is not essential for the process. In agreement with these results, depletion of profilin in *Xenopus* extracts by >98% has no effect on bacterial movement (Marchand *et al.*, 1995).

In the present work, we demonstrate that the first 234 amino acids of ActA (N-terminal domain) contain all of the elements necessary to induce actin tail formation and movement in *Xenopus* cytoplasmic extracts. In order to identify more precisely the regions of the N-terminal domain necessary for the actin polymerization process, a set of six ActA variants carrying small deletions in the N-terminal domain was constructed. Analysis of the ability of these ActA variants to induce actin tail formation, inhibition of the process with antibodies and *in vitro* experiments using synthetic peptides and purified G-actin or F-actin allowed the identification of two regions (spanning residues 21–97 and 117–121) critical for the actin-based motility. Based on these results, a hypothetical function for these two regions in actin tail formation is proposed.

Results

The N-terminal domain of ActA is sufficient to induce actin-based motility in Xenopus extracts

It was previously shown that the N-terminal domain of ActA is the only domain that is absolutely required for actin comet tail formation in infected cells (Lasa *et al.*, 1995). However, an ActA variant lacking both the central and the C-terminal domains and expected to trigger actin assembly was not associated with actin in infected cells, probably because part of the protein was embedded in the cell wall. In order to demonstrate that the N-terminal domain of ActA is sufficient to induce actin-based motility, we replaced the central and C-terminal domains of ActA by an unrelated protein to act as a spacer. We chose the ω domain of the β-galactosidase from *Escherichia coli* (Ullmann *et al.*, 1968) (Figure 1A). This domain is not involved in tetramer formation in the β-galactosidase enzyme (Jacobson *et al.*, 1994) and has nearly the same size (308 amino acids) as the ActA fragment that it replaces (346 amino acids). When expressed in a *L.monocytogenes* strain carrying a complete deletion of *actA* (Δ*actA*) (Figure 1B), the chimeric protein ActA(N)–LacZ induces the formation of comet tails in cytoplasmic extracts (Figure 1C). The percentage of bacteria associated with actin tails was equivalent to that formed with bacteria expressing the wild-type ActA (~25%). However, the size of the tails made by bacteria expressing the chimeric ActA(N)–LacZ protein were clearly shorter than those produced by bacteria expressing wild-type ActA, suggesting that they were moving more slowly [rapidly moving bacteria tend to be associated with longer comet tails (Theriot *et al.*, 1992)]. Using video-microscopy recordings of bacteria moving in cytoplasmic extracts, we found that bacteria expressing ActA(N)–LacZ protein moved at an average speed of 4.4 μm/min (n = 93, SD = 0.7), three times more slowly than bacteria expressing wild-type ActA (11.8 μm/min; n = 76, SD = 2.5).

To analyse the ability of ActA(N)–LacZ to cause actin assembly in infected cells, three types of cell lines were infected: macrophages (J774), Vero and PtK2 cells. After 5 h of infection, cells were fixed, F-actin was stained with FITC–phalloidin and bacteria were stained with rhodamine-labelled anti-ActA antibodies. In all three types of cell, bacteria expressing ActA(N)–LacZ were surrounded by F-actin and, in rare cases, very small actin comet tails were visible at one pole of some bacteria (data not shown). These bacteria did not form the microcolonies characteristic of the *L.monocytogenes* Δ*actA* strain (Kocks *et al.*, 1992), indicating that bacteria were moving in the cytoplasm of the infected cells, albeit very slowly (see Discussion).

As expected from transfection experiments (Pistor *et al.*, 1995) and from our results showing that, in the absence of the proline-rich domain of ActA, no VASP can be detected, immunolocalization experiments in cells infected with bacteria producing ActA(N)–LacZ did not reveal any VASP on the bacterial surface (data not shown). These results support the view that VASP is not absolutely essential for the ActA-mediated actin polymerization process.

Genetic analysis of the N-terminal domain of ActA: identification of two regions necessary for actin comet tail formation

In order to identify the regions in the N-terminal domain of ActA involved in the actin polymerization process, we generated several ActA variants in which small fragments of the N-terminal domain were deleted. The deletions

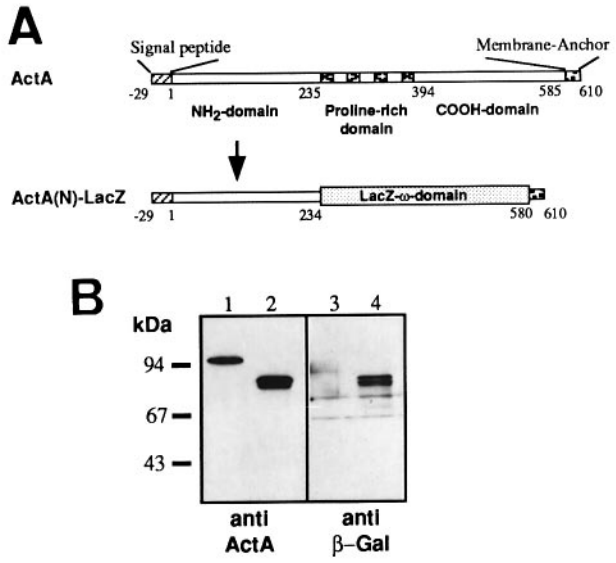

Fig. 1. Expression of the chimeric ActA(N)–LacZ protein in *L.monocytogenes*. (**A**) Schematic representation of the ActA protein and the chimeric protein ActA(N)–LacZ. The numbers indicate the position of the amino acids in the wild-type ActA protein, as described in Kocks *et al.* (1992). (**B**) Immunoblotting analysis of *L.monocytogenes* ΔactA transformed with: pActA3 (wild-type ActA) (lanes 1 and 3), pActA(N)–LacZ (lanes 2 and 4). Equivalent aliquots of total protein extracts were applied to an SDS–9% polyacrylamide gel. Separated proteins were transferred onto nitrocellulose and incubated with affinity-purified anti-ActA antibodies (A18K) (lanes 1 and 2) or polyclonal antibodies specific for the ω domain of β-galactosidase (lanes 3 and 4). (**C**) Movement of *L.monocytogenes* ΔactA expressing ActA(N)–LacZ in *Xenopus* extracts. The same field was observed every 3 min simultaneously by phase contrast to visualize the bacterium as a dark spot, and by fluorescence to show the bright rhodamine-labelled actin tails. The white arrow indicates the position of the bacterium, and the arrowhead indicates the position of the bacterium at time point zero.

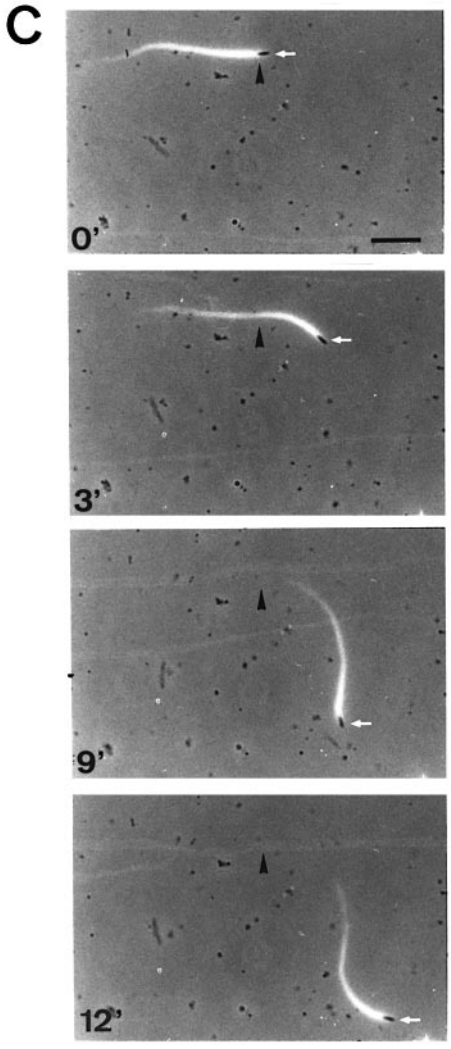


```
ActA     1 ATDSEDSSLNTDEWEE-----EKTEEQPSEVNTGPRY------ETAREVS
IactA  161 SNDDNDSRIDSDEWDDGEEAKEKVEEGKAEEGKAEEEKNNLGQEEISEAR

        40 SRDIKELEKSNKVRNTNKADLIAMLKEKAPKGPNINNNNSEQTENAAINE
       211 DRDLQELEKMGKVKNANVTALIAMLDSRAGKVARQDIKETLNDEVPAVLF

        90 EASGADRPAIQVERRHPGLPSDSAAEIKKRRKAIASS---DSELESLTYP
       261 HPKRSIKEILSDEQNRVPMNS---GKIKNRRKAIEGSDMEDSDMEDADTE

       137 DKPTKVNKKKVAKESVADASE---SDLDSSMQSADESSPQP-----LKANQQ
       308 EKPLAHGATGPLRTNNPSTSEETSEKIQSNENNEESSNQSQFDLISSSTE
```

Fig. 2. Alignment of amino acids in the N-terminal regions of ActA and IactA. Conserved amino acids are highlighted. Amino acids are numbered as in Kocks *et al.* (1992) for ActA and as in Gouin *et al.* (1995) for IactA.

were chosen on the basis of sequence comparisons between ActA and IactA, the homologous protein from *L.ivanovii* (Figure 2). Although the N-terminal domains of ActA and IactA do not show strong similarity (25% identity), there are two regions with high homology. The first region (116–123 amino acids) is rich in positively charged amino acids, the second region (41–64 amino acids) has 58% identity on a 23 amino acid overlap.

A schematic representation of the different ActA variants is shown in Figure 3A. As shown by immunoblotting of total protein extracts using anti-ActA affinity-purified antibodies (A18K), these proteins were well expressed in *L.monocytogenes* Δ*actA* strain and migrated with the expected motility (Figure 3C).

The ability of the different ActA variants to associate with polymerized actin was analysed in infected cells and in *Xenopus laevis* cytoplasmic extracts (Figure 3B). Two phenotypes were observed with respect to the actin polymerization process: either bacteria associated with actin without any visible comet tail; or bacteria associated with comet tails. Bacteria expressing ActA-$\Delta_{158–231}$ induced the formation of actin tails similarly to bacteria producing wild-type ActA in infected cells as well as in *Xenopus* extracts. Furthermore, the speed of movement was in the same range (11.1 μm/min; $n = 93$, SD = 0.7), indicating that this region (158–231) is not necessary for the process. In contrast, bacteria expressing ActA-$\Delta_{126–231}$, ActA-$\Delta_{114–231}$ and ActA-$\Delta_{97–231}$ were surrounded by F-actin, but actin comet tails were not visible. To address the role of a positively charged peptide (117-KKRRK-121) present in this region, in the actin polymerization process, we deleted these five amino acids. Bacteria expressing this protein variant (ActA-$\Delta_{116–122}$) were surrounded by F-actin, but were not able to produce actin comet tails, suggesting that this positively charged peptide is critical for actin tail

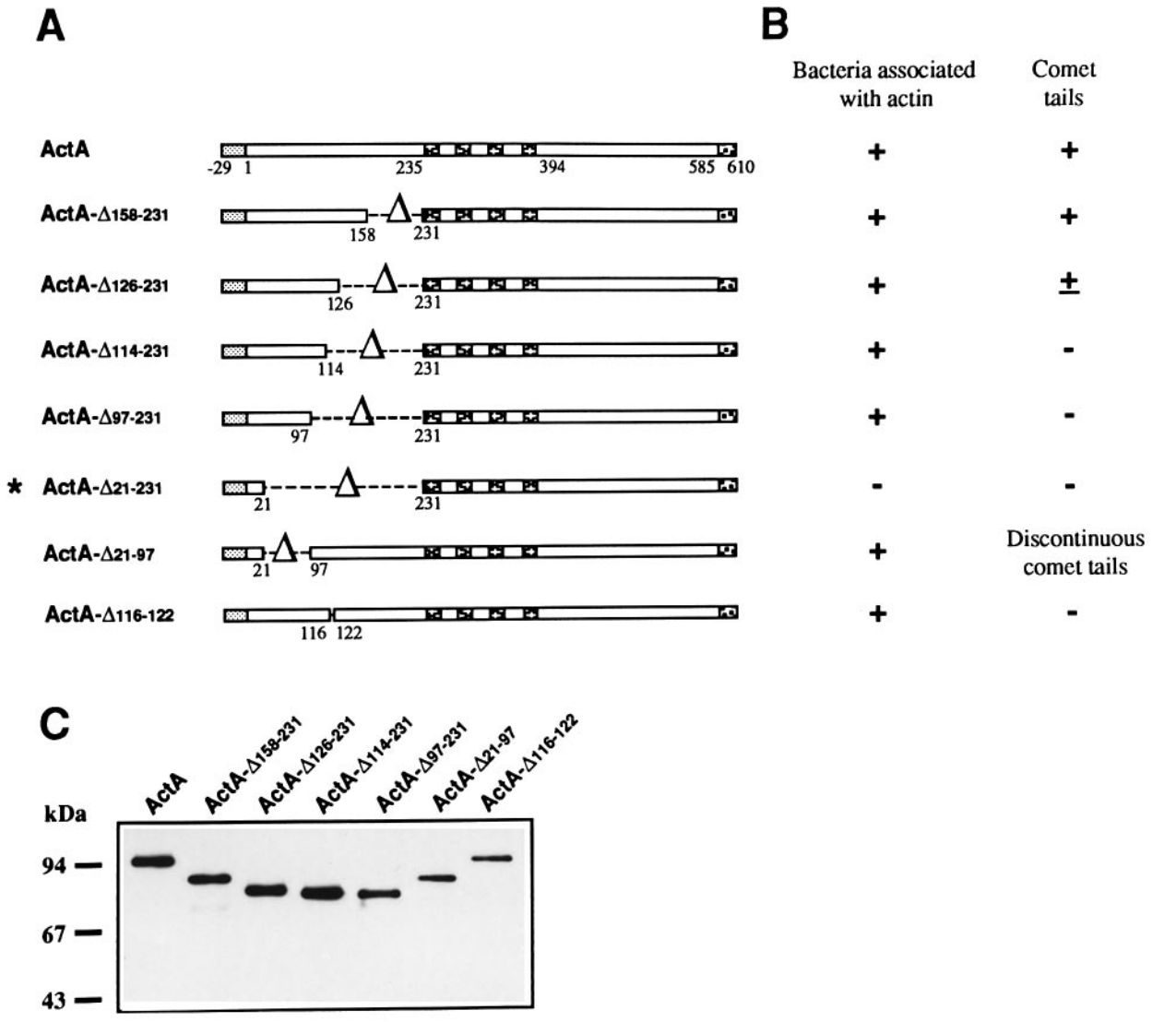

Fig. 3. Expression of ActA variants in *L.monocytogenes* and analysis of the ability to induce actin assembly. (**A**) Schematic representation of ActA variants. The numbers indicate the position of the amino acids in the wild-type protein. The dotted lines with a Δ correspond to the regions of ActA which have been deleted. All the constructs were expressed under the control of the actA promoter. They all contained the region coding for the signal peptide and the membrane anchor of ActA. *This construct has been published previously by Lasa *et al.* (1995). (**B**) Actin assembly phenotypes for each of the ActA variants are summarized. Three types of cells [macrophages (J774), Vero and PtK2] and *Xenopus* extracts were used to analyse the phenotypes. The ± symbol means that aberrant actin comet tails are rarely found in *Xenopus* extracts. (**C**) Immunoblot analysis of ActA variants expressed in *L.monocytogenes* ΔactA transformed with: (i) pActA3 (wild-type ActA), (ii) pActA-$\Delta_{158-231}$, (iii) pActA-$\Delta_{126-231}$, (iv) pActA-$\Delta_{114-231}$, (v) pActA-Δ_{97-231}, (vi) pActA-Δ_{21-97}, (vii) pActA-$\Delta_{116-122}$. Equivalent aliquots of total protein extracts were applied to an SDS–9% polyacrylamide gel. Separated proteins were transferred onto nitrocellulose and incubated with affinity-purified anti-ActA antibodies (A18K).

formation. To confirm this result, we made use of antibodies raised against a synthetic peptide covering residues 102–123 ($P_{102-123}$). Incubation of *L.monocytogenes* expressing wild-type ActA with increasing concentrations (0.1, 1 and 5 μg/ml) of affinity-purified anti-$P_{102-123}$ antibodies for 1 h strongly decreased the number of bacteria able to induce comet tails in *Xenopus* extracts (Figure 4). In contrast, incubation under the same conditions with antibodies raised against a synthetic peptide containing part of the first proline-rich repeat 235–252 (Y21T) had no significant effect on the ability of the bacteria to induce comet tails.

In a previous paper, we demonstrated that bacteria expressing ActA-Δ_{21-231} were not associated with F-actin (Lasa *et al.*, 1995). As shown in the present work, bacteria expressing ActA-Δ_{97-231} are still associated with F-actin, strongly suggesting that region 21–97 is also involved in the actin polymerization process. To address this issue, an ActA-Δ_{21-97} variant was produced. Bacteria expressing this protein were able to induce actin tails and movement in *Xenopus* extracts. However, the actin tails were strikingly discontinuous (Figure 5A). This phenomenon is analysed further in the next section.

Taken together, our results indicate that two regions within the N-terminal domain play a critical role in the actin-based motility. The region containing the peptide KKRRK (region T) is essential for actin tail formation, and a second region located between residues 21 and 97 (region C) is crucial for the continuity of the actin tail formation.

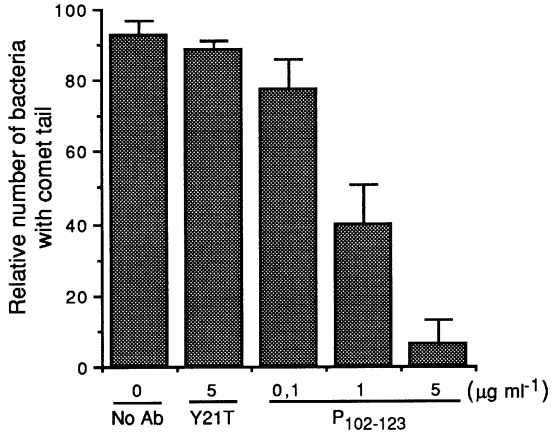

Fig. 4. Inhibition of actin tail formation in *Xenopus* extracts by antibodies specific to region T (117–121) of ActA. Bacteria expressing wild-type ActA were incubated with three different concentrations of affinity-purified antibodies against peptide $P_{102–123}$ which encompasses region T of ActA. As controls, bacteria were incubated either without antibody or with affinity-purified antibodies that recognize the first repeat of the proline-rich region (Y21T). Data are expressed as the percentage of bacteria associated with comets compared with the bacteria associated with actin. All values are mean ± SD from three independent experiments.

Analysis of the discontinuous actin tails produced by bacteria expressing ActA-$\Delta_{21–97}$

The movement of *L.monocytogenes* expressing wild-type ActA can be easily visualized under phase-contrast microscopy as phase-dense tails behind moving bacteria. Under these conditions, bacteria expressing ActA-$\Delta_{21–97}$ produced discontinuous phase-dense spots (Figure 5A). When phase contrast (to visualize bacteria) and fluorescence (to show rhodamine-labelled actin tails) were used simultaneously, we found that the phase-dense spots observed by phase contrast corresponded to the intensively stained spots observed by fluorescence microscopy (Figure 5A). Detailed analysis, in real time, of actin tail formation and movement showed that bacteria were first surrounded by a strongly fluorescent or phase-dense spot at their pole, while moving slowly (1.4 μm/min; n = 37; SD = 0.7). After this apparently rate-limiting step, the tail was elongated and the speed of the bacteria clearly increased (11.4 μm/min; n = 37; SD = 2.1). While bacteria were moving forward, the fluorescence intensity of the tail, as well as the speed of movement, decreased. Bacteria immediately began to be surrounded at their pole by an intensively stained spot, while remaining nearly immobile, and a new cycle of movement started (Figure 5B). Each complete cycle was achieved in ~55 s. We were interested in comparing the average rate of movement of bacteria expressing ActA-$\Delta_{21–97}$ with that of strains expressing wild-type ActA. The average speed of movement for bacteria expressing ActA-$\Delta_{21–97}$ was 7.2 μm/min (n = 51; SD = 1.8), almost half that of wild-type ActA (11.8 μm/min; n = 76; SD = 2.5).

Actin-binding properties of synthetic peptides corresponding to the regions of ActA important in actin recruitment and propulsion

One of the immediate questions emerging from our genetic analysis concerned the direct actin-binding properties of the identified ActA regions. To address this issue we first synthesized a peptide covering sequence 33–74 of ActA ($P_{33–74}$) and measured its actin-binding properties. Like thymosin β4 (Van Troys *et al.*, 1996), $P_{33–74}$ was able to inhibit salt-induced polymerization of Ca–G-actin in a concentration-dependent manner. Nearly complete inhibition was observed for more than 30 min when the peptide was added in a 20-fold molar excess over G-actin (Figure 6A). These data suggest that $P_{33–74}$ is able to bind G-actin. Peptide $P_{33–74}$ was also recovered in F-actin pellets obtained by airfuge centrifugation, indicating that it also binds to filamentous actin (Figure 6B). A shorter peptide covering residues 52–74 of ActA ($P_{52–74}$) displayed similar actin-binding properties, although higher concentrations of peptide were required to reach activities similar to that of $P_{33–74}$ (Figure 6B). A further truncated peptide, $P_{63–74}$, was inactive (data not shown), delineating the minimal actin-binding region to residues 33 and 63 of ActA.

In order to assess the specificity of the peptide activities, we synthesized a number of variants of $P_{52–74}$ that carried single amino acid substitutions scattered throughout the peptide. The activities of each of these variants were measured by inhibition of fluorescence (data not shown) and by sedimentation analysis (Figure 6C). Several of the variant peptides display weaker F-actin inhibitory activities, in particular those carrying substitutions L60G, L64G, K65E, K67E and K70E. These results are in line with the idea that region 53–65 could fold as an α-helix, while region 66–72 could adopt a highly charged coil structure. Indeed, these exchanges affect the helix stability (L60G and L64G) or reverse charge distributions in the loops (K65E, K67E and K70E) (Figure 6D). This situation could be similar to what was previously observed for thymosin β4, in which the actin-binding segment also consists of an α-helix followed by a highly charged loop region (Van Troys *et al.*, 1996).

The possible actin-binding properties of region T were studied using the synthetic peptide $P_{102–123}$ of ActA. When added to preformed actin filaments in increasing concentrations, we measured saturation of co-precipitation at a 20-fold molar excess (data not shown). Interestingly, the pellets showed a whitish appearance that was clearly different from the translucent nature of normally formed F-actin pellets. $P_{102–123}$ further induced actin precipitation when added to low-salt G-actin solutions. Since a similar effect was also observed with poly-L-lysine, we assume that the observed properties of $P_{102–123}$ could be due to the highly positively charged nature of the peptide. We therefore refrain from concluding that $P_{102–123}$ is a true actin-binding peptide, although at this stage there is little evidence to support the view that it is not.

Discussion

We provide here for the first time evidence that the N-terminal domain of ActA contains all the elements necessary to induce actin tail formation and movement. In addition, we have identified two peptide stretches involved in different steps of actin tail formation.

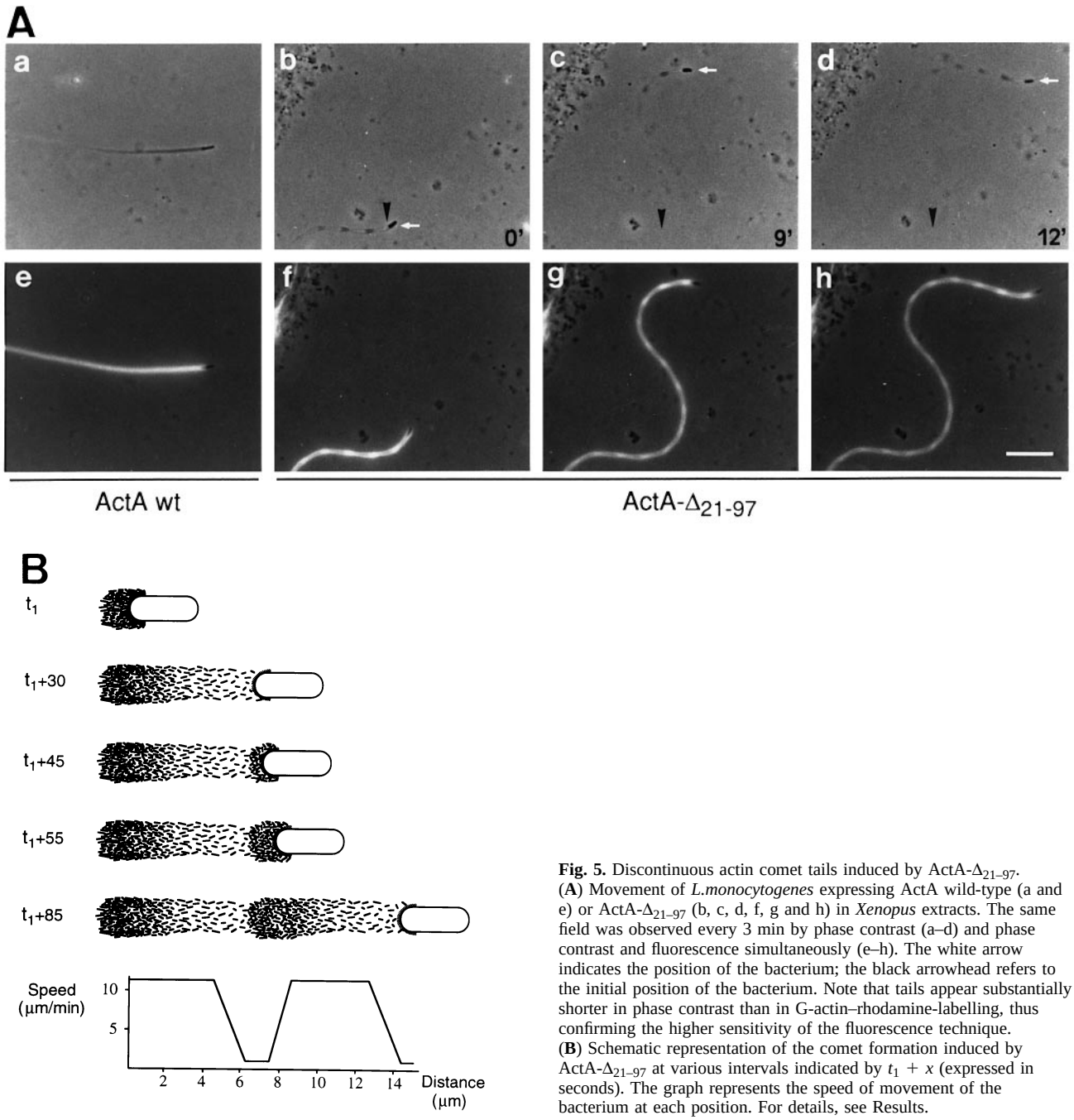

Fig. 5. Discontinuous actin comet tails induced by ActA-$\Delta_{21–97}$. (**A**) Movement of *L.monocytogenes* expressing ActA wild-type (a and e) or ActA-$\Delta_{21–97}$ (b, c, d, f, g and h) in *Xenopus* extracts. The same field was observed every 3 min by phase contrast (a–d) and phase contrast and fluorescence simultaneously (e–h). The white arrow indicates the position of the bacterium; the black arrowhead refers to the initial position of the bacterium. Note that tails appear substantially shorter in phase contrast than in G-actin–rhodamine-labelling, thus confirming the higher sensitivity of the fluorescence technique. (**B**) Schematic representation of the comet formation induced by ActA-$\Delta_{21–97}$ at various intervals indicated by $t_1 + x$ (expressed in seconds). The graph represents the speed of movement of the bacterium at each position. For details, see Results.

The N-terminal domain of ActA can by itself induce actin tail formation

We had previously shown that the first 234 amino acids of ActA were critical for actin-based motility (Friederich *et al.*, 1995; Lasa *et al.*, 1995). By using an ActA(N)–LacZ chimeric protein we demonstrate that the N-terminal domain is sufficient for actin-based motility in *Xenopus* cytoplasmic extracts, but actin tails with this construct were hardly observed in infected cells. It is now well established that filament disassembly in the actin tail is identical in all tests (Theriot *et al.*, 1992), which explains why faster-moving bacteria have longer tails. However, it has been noticed that, in *Xenopus* extracts, the average length of actin tails increases with time during incubation, which suggests that the efficiency of the depolymerization decreases, an event partially circumvented by the use of an ATP-regenerating system (creatine phosphate) (Marchand *et al.*, 1995). In contrast, inside cells, the average length of the tails does not increase with longer infection times, indicating that the efficiency of depolymerization does not change. Consequently, actin comet tails inside cells are not detectable if the rate of polymerization efficiency is only slightly higher than the depolymerization process. This is probably the case for the ActA(N)–LacZ construct. Indeed, bacteria expressing the chimeric ActA(N)–LacZ moved almost three times more slowly than bacteria expressing wild-type ActA, indicating that the efficiency of the polymerization process is relatively low. This inefficiency may be due to the lack of VASP

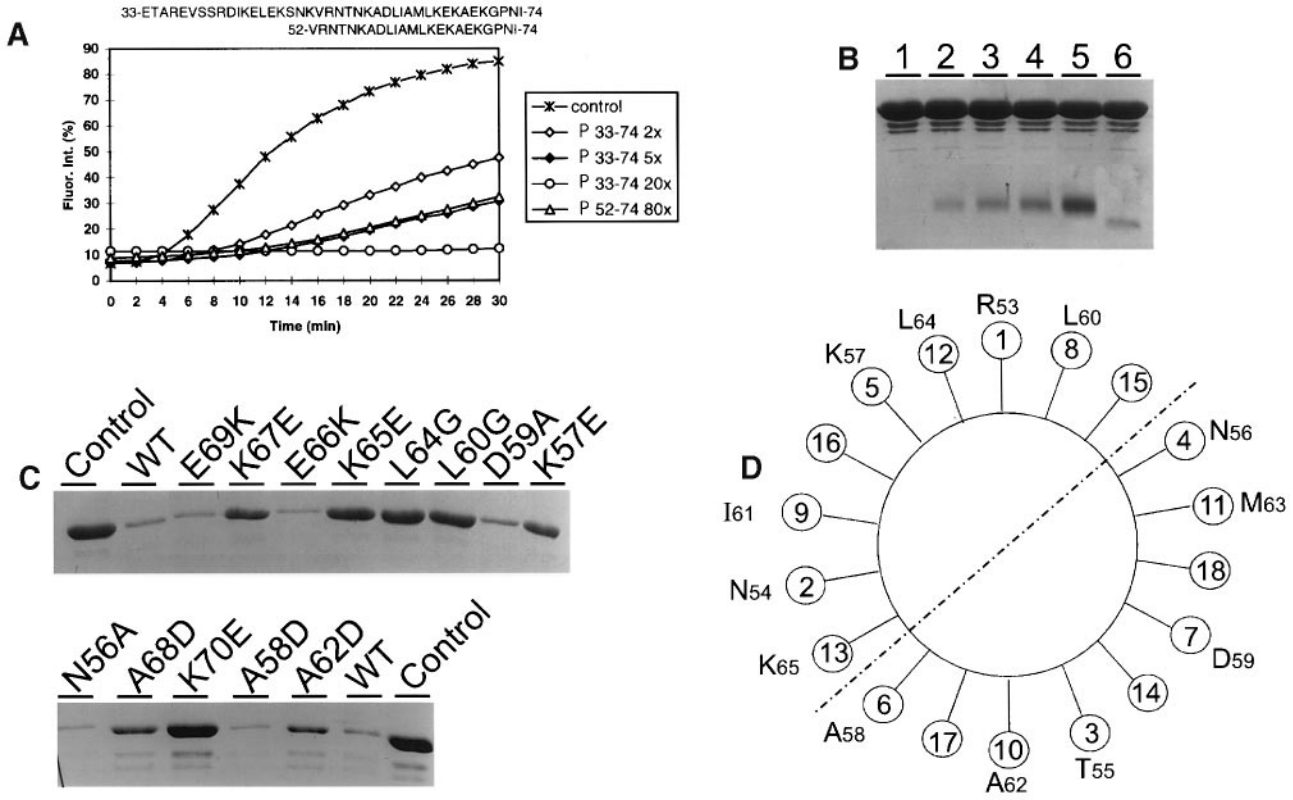

Fig. 6. Effects of synthetic peptides covering region C of ActA on actin polymerization. (**A**) Synthetic peptides covering region 33–74 ($P_{33–74}$) and 52–74 ($P_{52–74}$) in the ActA sequence inhibit actin polymerization. Salt (150 mM KCl and 1 mM $MgCl_2$) was added at time zero and the increase of fluorescence of pyrenyl-G-actin was measured for 30 min. The molar excess of each added peptide to actin is indicated. (**B**) Binding of peptide $P_{33–74}$ to preformed actin filaments. 24 μM actin was polymerized (lane 1) and to this was added peptide $P_{33–74}$ in 5× (lane 2), 10× (lane 3), 20× (lane 4) and 40× (lane 5) molar excess. The content of the pellets was analysed on mini slab gels. The upper band shows actin while the lower band represents the co-precipitated peptide. Lane 6 shows the same amount of F-actin to which was added a 40 M excess of peptide $P_{52–74}$.
(**C**) Sedimentation assay. F-actin pellets formed in the presence of peptide variants, recovered by airfuge centrifugation, were analysed on mini slab gels and stained with Coomassie blue. The control represents the amount of F-actin formed in the absence of peptide. WT refers to peptide $P_{52–74}$ added in 40 molar excess to the polymerizing mixture. Other samples show the precipitation data obtained with variants of peptide $P_{52–74}$ in which at each indicated site a single amino acid was replaced. (**D**) Helical wheel covering a three-turn α-helix extending from residues Arg53 (1) to Lys65 (13). When residues K57E, L60G, L64G, K65E and K67E located at the left side of the helix, were exchanged, this resulted in inhibition of activity. Exchanges in positions located at the right side of the helix (N56A, A58D, D59A and A62D) have no or little effect on the peptide's activity.

binding. Inside infected cells, VASP does not co-localize with bacteria expressing either ActA(N)–LacZ or ActA-ΔP (our unpublished results), strongly suggesting that binding of VASP, profilin and perhaps another unidentified protein, to the proline-rich repeats of ActA, is necessary to increase the efficiency of the actin polymerization process, but not that of actin comet tail formation. In terms of virulence, VASP probably plays a critical role by allowing actin-based cell–cell spreading.

Region T (117–121) is necessary for actin tail formation and region C (21–97) is necessary for continuous actin filament elongation

By transfection of mammalian cells with different ActA variants, Pistor *et al.* (1995) established that region 128–152 (numbering of amino acids as described in Domann *et al.*, 1992) or 99–123 (numbering as described in Kocks *et al.*, 1992), is essential for actin filament nucleation. However, their transfection assay could not distinguish between actin assembly and actin tail formation and movement. Our deletion analysis of the N-terminal domain of ActA in bacteria establishes the existence of two phenotypes with respect to the actin polymerization process: (i) bacteria surrounded with actin but unable to form comet tails; and (ii) bacteria associated with comet tails. These different phenotypes are associated with different regions of the N-terminal domain of ActA. Region T overlaps the residues previously identified by the 'mitochondrial targeting assay' (Pistor *et al.*, 1995) and is responsible for an efficient actin polymerization process leading to the actin tail formation. In its absence, bacteria are associated with F-actin but are unable to produce actin tails.

The fact that bacteria expressing ActA-$\Delta_{97–231}$ were still associated with F-actin, while bacteria expressing ActA-$\Delta_{21–231}$ were not (Lasa *et al.*, 1995), strongly suggested that a second region covering residues 21–97 was able to induce actin polymerization, or at least was able to recruit F-actin. In agreement with this idea, bacteria expressing an ActA variant, in which the region between amino acids 21 and 97 was deleted (ActA-$\Delta_{21–97}$), induced actin comet tails, albeit discontinuously, as if formation of actin tail in this mutant was due to periodic cycles of starting and stalling. Therefore, region C also plays a role in the actin assembly process.

Although previous attempts to demonstrate interactions between ActA and G-actin–ATP or F-actin have failed, *in vitro* experiments with a synthetic peptide containing

residues 33–74 demonstrated that this region is able to bind F-actin. One possible explanation is that, in ActA, region 33–74 may be shielded. The case of ActA would be similar to that of vinculin, a 1066 amino acid protein containing a N-terminal globular head and a C-terminal rod-like domain connected by a short proline-rich motif. As recently established, full-length vinculin interacts with its ligands (F-actinin, α-actinin, talin, phospholipids) less efficiently than each of its isolated domains (for review, see Jockusch and Rüdiger, 1996), indicating that in the intact molecule, the ligand-binding sites are not always in an active form. In the case of vinculin, the factors involved in the conformational switches seem to be a cooperative combination of phosphorylation, binding of PtdIns(4,5)P2 and binding of the various protein ligands. In the case of ActA, phosphorylation (Brundage *et al.*, 1993) and/or ligand binding (VASP) (Chakraborty *et al.*, 1995) could induce a similar functional switch and unshield either actin binding sites or binding of intermediate proteins which stimulate actin binding.

Towards a model of actin assembly by the N-terminal domain of ActA

How can one explain the continuous actin polymerization process induced by ActA? Also, how can the discontinuous actin tail formation induced by ActA-$\Delta_{21–97}$ be explained? We have to take into account three sets of data. First, that nucleation (assembly of three monomers of actin to form a trimer) is the rate-limiting step for actin polymerization (Pollard and Cooper, 1986); the next step, elongation (addition of actin monomers to the trimers, resulting in filament formation) occurs rapidly once nucleation has taken place. Second, that electron micrographs of actin comets produced by *L.monocytogenes* show that filaments in the tails are short (0.2 μm) and oriented with their barbed ends (fast-growing) towards the bacteria (Tilney *et al.*, 1992). It has been proposed that, while continuous nucleation takes place, filament elongation may be terminated by barbed end-capping proteins, followed by cross-linking of the filaments (Tilney and Tilney, 1993). A tail is thus the result of nucleation, elongation, capping, release and cross-linking. Third, that thermodynamic studies have established that actin assembly results from the local maintenance of uncapped filament barbed ends at the bacterium surface (Marchand *et al.*, 1995).

Based on these data, we propose that region T is more specifically involved in elongation/tail formation and region C in maintaining the barbed ends uncapped, thereby allowing continuous filament elongation. If we consider that propulsion of the bacteria is due to elongation of a critical minimum number of actin filaments, in bacteria expression wild-type ActA, the filaments lost for the elongation process by capping are constantly replaced by newly nucleated filaments. Since the rates of capping and nucleation do not vary, at least over short intervals, the F-actin concentration in the tails appears relatively homogeneous (while in fact exponentially diminishing) and the speed of movement constant. In the absence of region C (21–97) the newly nucleated filaments may be protected less efficiently from the capping proteins and the nucleation process cannot overcome the loss of free barbed ends due to capping. When the number of uncapped filaments implicated in the elongation process is not sufficient to propel the bacteria, the speed of movement decreases. During this lag time ActA continues the slow process of nucleation of new filaments until accumulation of a critical number of newly nucleated filaments (phase-dense spots) is reached. Elongation of the newly synthesized filaments can then propel the bacteria at high speed, but unprotected filaments begin to be capped again and a new cycle begins.

If this model is correct, increasing the concentration of capping proteins should reproduce the discontinuous tail phenotype in bacteria expressing ActA wild-type. We are currently testing this hypothesis. In fact, in rare cases (our unpublished observations), bacteria expressing wild-type ActA also make discontinuous actin comet tails in *Xenopus* extracts, suggesting that the concentration of actin-capping proteins may vary in some areas of the extracts, or that spontaneous mutations may arise in the C region.

In the future, the identification of host cell factors that interact with or modify the specific regions of ActA identified here should help to reconstitute a minimal *in vitro* system allowing actin-based motility.

Materials and methods

Construction of the ActA(N)–LacZ chimeric protein

The ω domain of β-galactosidase was amplified from pMC1871 (Pharmacia Biotech) using the following primers: (5′-GG**GGTACC**G-AACGCGACCGCA-3′) (703), (5′-GG**CCCGGG**CGCTCAGCTG-GAA-3′) (1011) (the 5′-end primer contains a *Kpn*I restriction site and the 3′-end a *Xma*I site). The number in parentheses for each primer corresponds to the position of the last amino acid encoded by the PCR fragment in the mature protein.

After digestion with *Kpn*I–*Xma*I, the PCR product was cloned in pActA-ΔPC (Lasa *et al.*, 1995) digested with the same restriction enzymes.

Construction of deletions in the N-terminal domain of ActA

We generated a series of N-terminal fragments of *actA* by PCR. We used the same 5′-end primer (209 bp upstream from the first nucleotide of the initiating codon) containing an *Eco*RI restriction site (5′-**GGAAT-TC**AGTTGGGGTTAACT-3′). For the 3′-end, the following primers containing a *Kpn*I restriction site were used:

(5′-G**GGTACC**GCACTTTCAGAAGCATC-3′) (158);
(5′-G**GGTACC**GATGATGCTATGGC-3′) (126);
(5′-G**GGTACC**GCTGCGCTATCCGA-3′) (114);
(5′-G**GGTACC**GCTGGTCGGTCGGCT-3′) (97).

All these PCR fragments were digested with *Eco*RI–*Kpn*I and cloned into pActA-ΔN (Lasa *et al.*, 1995) digested with the same enzymes. The number in parentheses corresponds to the position of the last amino acid encoded by the PCR fragment in the mature ActA, as described by Kocks *et al.* (1992).

For the construct ActA-$\Delta_{21–97}$, a fragment containing part of the N-terminal domain was produced using the following primers:

5′-end (5′-GG**GGTACC**AGCTATACAAGTG-3′) (97);
3′-end (5′-GG**CCCGGG**AAGCATTTACCTCTTC-3′) (234).

This fragment digested with *Kpn*I–*Xma*I was cloned into pActA-ΔN digested with the same restriction enzymes.

Deletion of five amino acids to produce construct ActA-$\Delta_{116–122}$ was done using an oligonucleotide-directed mutagenesis system (Sculptor™ IVM system, Amersham). A fragment containing the N-terminal domain of ActA from pActA-ΔPC (Lasa *et al.*, 1995) was digested with *Eco*RI–*Kpn*I and cloned into appropriately digested M13mp19. Mutagenesis was performed using the oligonucleotide 5′-CCGATGATGCTATG-GCAATTTCCGCTGCGCTA-3′, which deleted the sequence coding for the five amino acids. Following mutagenesis, the sequence of the entire fragment was determined. Recombinants harbouring the desired mutations were digested with *Eco*RI–*Kpn*I and cloned into pActA-ΔN.

The resulting plasmids were electroporated into *L.monocytogenes* LO28 Δ*actA* (Gouin *et al.*, 1995) as described by Lasa *et al.* (1995) obtaining the following strains: ActA-$\Delta_{158–231}$ (BUG1368), ActA-

$\Delta_{126–231}$ (BUG1370), ActA-$\Delta_{114–231}$ (BUG1372), ActA-$\Delta_{97–231}$ (BUG1374), ActA-$\Delta_{21–97}$ (BUG1374) and ActA-$\Delta_{116–122}$ (BUG1378). The constructs were verified by sequence determination using the T7 sequencing kit (Pharmacia Biotech). Stable expression of the proteins was analysed by immunoblotting as described (Lasa *et al.*, 1995).

Cell culture, infection and double fluorescence labelling of bacteria and associated F-actin

The mouse macrophage-like cell line J774 (ECACC 85011428), the Vero cell line (ATCC CRL1587) and the *Potoroo* kidney epithelial PtK2 cells (ATCC CCL56) were cultured as described by Dramsi *et al.* (1993), Kocks *et al.* (1993) and Gouin *et al.* (1995), respectively.

Immunofluorescence of *L.monocytogenes*-infected cells was performed as described by Lasa *et al.* (1995). Preparations were observed in a laser scanning confocal microscope (Wild Leitz) or an epifluorescence microscope (Optiphot-2, Nikon).

Antibodies

Polyclonal antibodies against β-galactosidase recognizing the ω domain (Celada *et al.*, 1974) were generously provided by A.Ullmannn. Polyclonal antibodies recognizing VASP (Reinhard *et al.*, 1992) were generously provided by U.Walter. The ActA-specific affinity-purified polyclonal antibodies were produced either against a synthetic peptide comprising the first 18 N-terminal residues of mature ActA (A18K) (Friederich *et al.*, 1995), against a synthetic peptide comprising part of the first proline-rich repeat (Y21T) (Kocks *et al.*, 1993) or against a peptide $P_{102–123}$ (CERRHPGLPSDSAAEIKKRRKAI) covering residues 102–123 from ActA (this work). Affinity purification of the antibodies was done as described by Friederich *et al.* (1995).

Analysis of motility of L.monocytogenes derivatives

For analysis of the motility of *L.monocytogenes* derivatives expressing ActA variants in cytoplasmic extracts of *Xenopus laevis* eggs and inhibition of actin tail formation with antibodies, interphasic extracts of *Xenopus* eggs were prepared as described (Marchand *et al.*, 1995). Bacterial strains were prepared and motility assays were preformed as described (Lasa *et al.*, 1995) with the following modifications: extracts mixed with bacteria were incubated for 1 h at room temperature, compressed between a slide and a coverslip and incubated for a further 2 h. The preparations were observed with a Zeiss Axiovert 135 microscope equipped with CCD 5405 camera (Hamamatsu) which allowed simultaneous visualization of bacteria by phase contrast, and actin tails by fluorescence. Images were recorded in real time or in time-lapse on a video tape recorder. An ARGUS-20 image processor (Hamamatsu) attached to a Macintosh computer was used to analyse the movement of bacteria.

For inhibition of actin comet tail formation, 10 µl of bacteria solution (10^9 bacteria/ml) resuspended in *Xenopus* buffer (100 mM KCl, 1 mM $MgCl_2$, 0.1 mM $CaCl_2$, 50 mM sucrose in 10 mM HEPES pH 7.7) were incubated for 1 h with 0.1, 1 and 5 µg/ml of affinity-purified antibodies diluted in the same buffer. 1 µl of this solution was then mixed with 10 µl of *Xenopus* extract supplemented with 1 mM Mg-ATP, 30 mM creatine phosphate and 3 µM rhodamine-labelled G-actin (cytoskeleton). After 1 h incubation, 2 µl were compressed between a slide and a 22×22 mm coverslip, and incubated for a further 2 h before observation by microscopy.

Peptides

Peptides were synthesized on a model 431 A peptide synthesizer (Applied Biosystems Inc., Foster City, CA) on *p*-hydroxymethyl resin using the F-moc chemistry procedure following the manufacturer's instructions. After cleavage, the peptide–resin was conjugated with trifluoroacetic acid (TFA), the peptide was precipitated with *t*-methyl-butyl ether and collected by centrifugation at 2000 *g*. The residue was dried for 2 h in a Speedvac and then redissolved in water and adjusted to pH 8 with 4 M NaOH. Peptides were desalted over a Sephadex G25 column in water. The eluate was monitored by UV absorbance at 254 nm. Peptide fractions were collected, lyophilized and further purified by preparative HPLC on a C4 reverse-phase column. The purified peptides were desalted once more as described above and their concentrations determined after alkaline hydrolysis followed by ninhydrin staining (Hirs, 1967).

Actin polymerization and binding assays

Rabbit skeletal muscle actin was prepared following the procedure of Spudich and Watt (1971) and isolated as Ca–G-actin by chromatography over Sephadex G-200 in G-buffer (5 mM Tris–HCl pH 7.7, 0.1 mM $CaCl_2$, 0.2 mM ATP, 0.2 mM dithiothreitol). Actin was labelled with *N*-(1-pyrenyl) iodoacetamide as described (Kouyama and Michashi, 1981). Actin polymerization in the presence of peptides was measured by the increase in fluorescence of pyrenyl–actin (Brenner and Korn, 1983). Peptides, dissolved in G-buffer at the indicated concentrations, were mixed at room temperature with 12 µM of G-actin of which 10% was pyrenyl-labelled. Polymerization was initiated 10 min later by the addition of salt (final concentration 150 mM KCl and 1 mM $MgCl_2$). The increase in fluorescence was monitored at room temperature as a function of time with a SFM25 fluorimeter (Kontron Instruments, Zurich) using excitation and emission wavelengths of 305 nm and 388 nm respectively. Fluorescence could be measured continuously for at least 20 min without noticeable bleaching of the sample.

Actin polymerization was also studied by a sedimentation assay. Peptides were incubated with G-actin (24 µM) at room temperature in G-buffer, salt was added. The F-actin formed after 30 min of incubation was sedimented for 15 min at 30 p.s.i. in a Beckman airfuge (Beckman Instruments). The supernatant was discarded and the pellet washed twice with F-buffer and resuspended in 60 µl of gel sample buffer and an aliquot analysed by gel electrophoresis on mini-slab gels.

Binding of the peptides to preformed actin filaments was carried out with F-actin formed in the presence of 150 mM KCl and 1 mM $MgCl_2$ and the addition of the indicated amounts of peptide 15 min after actin polymerization. The pellets collected after centrifugation were analysed by SDS–PAGE.

Acknowledgements

We wish to thank T.Pugsley and K.Ireton for critical reading of the manuscript, R.Hellio for help in the confocal analysis and the Service de Photographie de l'Institut Pasteur for photograph assistance. We thank M.F.Carlier, D.Pantaloni and J.B.Marchand for stimulating discussions, M.Bornens and A.Paoletti for help with *Xenopus* egg extracts, T.Hyman for helpful advice with the video microscopy equipment, A.Ullmannn for advice and anti-β-galactosidase antibodies, and U.Walter for anti-VASP antibodies. I.L. is a recipient of a post-doctoral fellowship from the EEC (Training and Mobility of Researchers). This study received financial support from the ARC (CT1164), the Ministère de la Recherche (ACC-SV6), EEC (BMH4 CT 96-0659), EEC (CHRX CT 94-0430), VLAB-COT 035, GOA (91/96-3) to J.V., from the Flemish Community and the Pasteur Institute.

References

Brenner,S.L. and Korn,E.D. (1983) On the mechanism of actin monomer-polymer subunit exchange at steady state. *J. Biol. Chem.*, **258**, 5013–5020.

Brundage,R.A., Smith,G.A., Camilli,A., Theriot,J. and Portnoy,D.A. (1993) Expression and phosphorylation of the *Listeria monocytogenes* ActA protein in mammalian cells. *Proc. Natl Acad. Sci. USA*, **90**, 11890–11894.

Celada,F., Ullmannn,A. and Monod,J. (1974) An immunological study of complementary fragments of β-galactosidase. *Biochemistry*, **13**, 5543–5547.

Chakraborty,T. *et al*. (1995) A focal adhesion factor directly linking intracellularly motile *Listeria monocytogenes* and *Listeria ivanovii* to the actin-based cytoskeleton of mammalian cells. *EMBO J.*, **14**, 1314–1321.

Cossart,P. (1995) Bacterial actin based motility. *Curr. Opin. Cell Biol.*, **7**, 94–101.

Cudmore,S., Cossart,P., Griffiths,G. and Way,M. (1995) Actin-based motility of vaccinia virus. *Nature*, **378**, 636–638.

Domann,E., Wehland,J., Rohde,M., Pistor,S., Hartl,M., Goebel,W., Leimeister-Wächter,M., Wuenscher,M. and Chakraborty,T. (1992) A novel bacterial gene in *Listeria monocytogenes* required for host cell microfilament interaction with homology to the proline-rich region of vinculin. *EMBO J.*, **11**, 1981–1990.

Dramsi,S., Kocks,C., Forestier,C. and Cossart,P. (1993) Internalin-mediated invasion of epithelial cells by *Listeria monocytogenes* is regulated by the bacterial growth state, temperature and the pleiotropic activator, *prfA*. *Mol. Microbiol.*, **9**, 931–941.

Friederich,E., Gouin,E., Hellio,R., Kocks,C., Cossart,P. and Louvard,D. (1995) Targeting of *Listeria monocytogenes* ActA protein to the plasma membrane as a tool to dissect both actin-based cell morphogenesis and ActA function. *EMBO J.*, **14**, 2731–2744.

Gouin,E., Dehoux,P., Mengaud,J., Kocks,C. and Cossart,P. (1995) *iactA* of *Listeria ivanovii* although distantly related to *Listeria monocytogenes actA* restores actin tail formation in a *L. monocytogenes actA* mutant. *Infect. Immun.*, **63**, 2729–2737.

Hirs,C.H.W. (1967) Detection of peptides by chemical methods. *Methods Enzymol.*, **11**, 325–329.

Jacobson,R.H., Zhang,X.J., DuBose,R.F. and Matthews,B.W. (1994) Three-dimensional structure of β-galactosidase from *E. coli*. *Nature*, **369**, 761–766.

Jockusch,B. and Rüdiger,M. (1996) Crosstalk between cell adhesion molecules: vinculin as a paradigm for regulation by conformation. *Trends Cell Biol.*, **6**, 311–315.

Kocks,C., Gouin,E., Tabouret,M., Berche,P., Ohayon,H. and Cossart,P. (1992) *Listeria monocytogenes*-induced actin assembly requires the *actA* gene product, a surface protein. *Cell*, **68**, 521–531.

Kocks,C., Hellio,R., Gounon,P., Ohayon,H. and Cossart,P. (1993) Polarized distribution of *Listeria monocytogenes* surface protein ActA at the site of directional actin assembly. *J. Cell Sci.*, **105**, 699–710.

Kocks,C., Marchand,J.B., Gouin,E., d'Hauteville,H., Sansonetti,P.J., Carlier,M.F. and Cossart,P. (1995) The unrelated surface proteins ActA of *Listeria monocytogenes* and IcsA of *Shigella flexneri* are sufficient to confer actin-based motility to *L. innocua* and *E. coli* respectively. *Mol. Microbiol.*, **18**, 413–423.

Kouyama,T. and Michashi,K. (1981) Fluorimetry study of *N*-(1-pyrenyl)iodoacetamide-labelled F-actin. *Eur. J. Biochem.*, **114**, 33–38.

Kreft,J., Dumbsky,M. and Theiss,S. (1995) The actin polymerization protein from *Listeria ivanovii* is a large repeat protein which shows only limited amino-acid sequence homology to ActA from *Listeria monocytogenes*. *FEMS Microbiol. Lett.*, **126**, 113–122.

Lasa,I. and Cossart,P. (1996) Actin-based motility: towards a definition of the minimal requirements. *Trends Cell Biol.*, **6**, 109–114.

Lasa,I., David,V., Gouin,E., Marchand,J. and Cossart,P. (1995) The amino-terminal part of ActA is critical for the actin based motility of *Listeria monocytogenes*; the central proline-rich region acts as a stimulator. *Mol. Microbiol.*, **18**, 425–436.

Lett,M.C., Sasakawa,C., Okada,N., Sakai,T., Makino,S., Yamada,M., Komatsu,K. and Yoshikawa,M. (1989) *virG*, a plasmid-coded virulence gene of *Shigella flexneri*: identification of the *virG* protein and determination of the complete coding sequence. *J. Bacteriol.*, **171**, 353–359.

Marchand,J.B., Moreau,P., Paoletti,A., Cossart,P., Carlier,M.F. and Pantaloni,D. (1995) Actin-based movement of *Listeria monocytogenes* in *Xenopus* egg extracts is due to local uncapping of the barbed ends of actin filaments at the bacterial surface and resulting shift in steady state of actin assembly. *J. Cell Biol.*, **130**, 331–343.

Pantaloni,D. and Carlier,M.F. (1993) How profilin promotes actin filament assembly in the presence of thymosin β4. *Cell*, **75**, 1007–10014.

Pistor,S., Chakraborty,T., Niebuhr,K., Domann,E. and Wehland,J. (1994) The ActA protein of *L. monocytogenes* acts as a nucleator inducing reorganization of the actin cytoskeleton. *EMBO J.*, **13**, 758–763.

Pistor,S., Chakraborty,T., Walter,U. and Wehland,J. (1995) The bacterial actin nucleator protein ActA of *Listeria monocytogenes* contains multiple binding sites for host microfilament proteins. *Curr. Biol.*, **5**, 517–525.

Pollard,T.D. and Cooper,J.A. (1986) Actin and actin-binding proteins. A critical evaluation of mechanisms and functions. *Annu. Rev. Biochem.*, **55**, 987–1035.

Reinhard,M., Halbrügge,M., Scheer,U., Wiegand,C., Jockusch,B.M. and Walter,U. (1992) The 45/50 kDa phosphoprotein VASP purified from human platelets is a novel protein associated with actin filaments and focal contacts. *EMBO J.*, **11**, 2063–2070.

Reinhard,M., Giehl,K., Abel,K., Haffner,C., Jarchau,T., Hoppe,V., Jockusch,B.M. and Walter,U. (1995) The proline-rich focal adhesion and microfilament protein VASP is a ligand for profilins. *EMBO J.*, **14**, 1583–1589.

Sanger,J., Mittal,B., Southwick,F.S. and Sanger,J.P. (1995) *Listeria monocytogenes* intracellular migration: inhibition by profilin, vitamin, D-binding protein and DNase I. *Cell Motil. Cytoskeleton*, **30**, 38–49.

Smith,G.A., Portnoy,D.A. and Theriot,J.A. (1995) Asymmetric distribution of the *Listeria monocytogenes* ActA protein is required and sufficient to direct actin-based motility. *Mol. Microbiol.*, **17**, 945–951.

Spudich,J.A. and Watt,S. (1971) Regulation of rabbit skeletal muscle contraction. *J. Biol. Chem.*, **246**, 4866–4871.

Theriot,J. (1995) The cell biology of infection by intracellular bacterial pathogens. *Annu. Rev. Cell Dev. Biol.*, **11**, 213–239.

Theriot,J.A., Mitchison,T.J., Tilney,L.G. and Portnoy,D.A. (1992) The rate of actin-based motility of intracellular *Listeria monocytogenes* equals the rate of actin polymerization. *Nature*, **357**, 257–260.

Theriot,J.A., Rosenblatt,J., Portnoy,D.A., Goldschmidt-Clermont,P.J. and Mitchison,T.J. (1994) Involvement of profilin in the actin-based motility of *L. monocytogenes* in cells and in cell-free extracts. *Cell*, **76**, 505–517.

Tilney,L.G. and Tilney,M.S. (1993) The wily ways of a parasite: induction of actin assembly by *Listeria*. *Trends Microbiol.*, **1**, 25–31.

Tilney,L.G., DeRosier,D.J., Weber,A. and Tilney,M.S. (1992) How *Listeria* exploits host cell actin to form its own cytoskeleton. II. Nucleation, actin filament polarity, filament assembly, and evidence for a pointed end capper. *J. Cell Biol.*, **118**, 83–93.

Ullmannn,A., Jacob,F. and Monod,J. (1968) On the subunit structure of wild-type versus complemented β-galactosidase of *Escherichia coli*. *J. Mol. Biol.*, **32**, 1–32.

Van Troys,M., Dewitte,D., Goethals,M., Carlier,M.F., Vandekerckhove,J. and Ampe,C. (1996) The actin binding site of thymosin β-4 mapped by mutational analysis. *EMBO J.*, **15**, 201–210.

Received on October 29, 1996; revised on November 21, 1996